Optica Applicata, Vol. XLIV, No. 3, 2014
DOI: 10.5277/oa140303

A new design of a photonic crystal fiber with a beam shaping effect and flexible management of dispersion and confinement loss

YUCHUN HUANG, PING JIANG*, HUAJUN YANG, MINGYIN YU

School of Physical Electronics, University of Electronic, Science and Technology of China, Chengdu 610054, China

*Corresponding author: jiangp@uestc.edu.cn

A new design of a guiding-index photonic crystal fiber which possesses a beam shaping effect and flexible control of dispersion has been proposed in this paper. It can shape a Gaussian beam into a circular hollow beam with certain dimension, which can be used in optical communication systems with a Cassegrain antenna to improve transmission efficiency by avoiding the loss of energy caused by the subreflector center reflection. In addition, its dispersion and confinement loss can be changed in a broad range by slightly adjusting structural parameters under condition that the hollow beam dimension remains about the same. Fairly practical properties, zero dispersion or flattened dispersion, can be obtained when structural parameters are set appropriately. A series of models with different parameters are analyzed and compared. Results of numerical simulation show that the ultra-low dispersion of 1.802 ps/km/nm can be obtained when $\lambda = 1.31$ μm. Several modest design parameters are given as well.

Keywords: photonic crystal fiber, hollow beam, chromatic dispersion.

1. Introduction

Photonic crystal fiber (PCF) [1] is a novel kind of an optical fiber whose clad is composed of air holes running along its length. Since its first fabrication in 1996 [1], PCF has attracted considerable attention because of excellent propagation properties. It has exhibited extraordinary features such as a wide range of single-mode operations [2], easily controllable dispersion [3, 4], birefringence [5, 6], and tailorable effective mode area [7, 8]. Strong potential has been shown in nonlinear fiber optics such as the generation of a super-continuum [9] and in many other novel fiber devices [10]. What is more, a flexible and precise management of chromatic dispersion in a broad spectral range makes it receive wide attention in applying in optical communication, such as coping with ever-increasing data rate and spectral density of wavelength division multiplexing (WDM) channels [11].

Many designs have been proposed to engineer chromatic dispersion in PCF. Some researches transform material to achieve it by doping the core area [12, 13] or filling the cladding air holes with liquid [14], other researches vary structures by employing special shaped air holes [15, 16] instead of circular air holes. Flattened or near-to-zero dispersion characteristics can be obtained. In some cases, a special ring-shaped beam, usually hexagonal or square, can be generated as a by-product [17]. However, on one side, these polygonal ring-shaped beams cannot apply to some optical systems perfectly. For example, in the optical communication systems with a Cassegrain antenna, to avoid the loss of energy caused by the subreflector center reflection [18], a circular hollow beam [19] works more efficiently than those polygonal ring-shaped beams. On the other side, a change in structure parameters aiming at a proper beam size may deteriorate the dispersion characteristics.

In this paper, a novel large-mode-area PCF with a coaxial ring-shaped defect in the air hole clad is constructed based on the index guiding principle. The design details of the PCF are proposed in this paper and numerical analysis has been elaborated. The modes of the proposed fiber are analyzed by the finite element method (FEM). The results of simulation with the analysis and comparison covering electric field distribution, beam dimension, chromatic dispersion and confinement loss have been presented. The proposed fiber can be used in space optical communication systems to greatly enhance the transmission efficiency. And a good management of chromatic dispersion can be achieved under the premise that the beam size and type remain the same.

2. Design method and numerical analysis

As a new kind of optical fiber, PCF consists of a core and clad, obeying the propagation law of total internal reflection, which is similar to a traditional optical fiber. PCF is made up of unitary material, whose clad is a microstructure built by punching sub-micrometer air holes tightly and periodically. It can be sorted to two types according to distinct structures: index-guiding PCF [20] and band-gap PCF. The core of index-guiding PCF is composed of host material, hence the refractive index of the core is higher than that of the clad. The new designed structure proposed in this paper exactly belongs to this type.

The optical beam with zero central intensity is called a hollow beam (HB). Conventional geometry [17, 21, 22] of PCF was always built based on a hexagonal or triangular lattice, thus the cross-section of the core is a hexagon or hexagonal ring actually. On the contrast, the air holes are arranged in a series of concentric circular rings regularly in the proposed PCF, whose cross-section is shown in Fig. 1**a**. To produce HB, a new structure is designed, which is shown in Fig. 1**b**. The host material is fused silica. Several layers of the air holes are removed to form an annular core, and the light can propagate in this area whose refractive index is higher than in the rest region of the fiber. The air hole pitch Λ, the distance between any two adjacent layers is 1.2 μm and the radius of the air hole r is 0.4 μm. Obviously, an annular core of the new design is a circular ring. While, a hexagonal ring-shaped core can be obtained

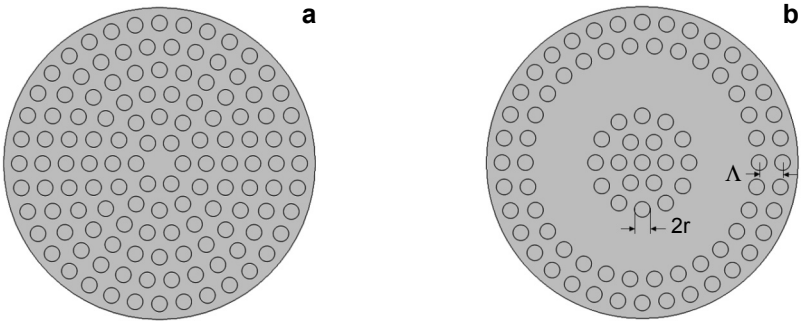

Fig. 1. Cross-section of new proposed PCF (see text for explanation).

when a similar removing method is applied to conventional geometry. The difference between them may cause distinct field distribution of a propagating beam, which will be particularly discussed in the simulation section.

Chromatic dispersion is an essential indicator when estimating a nonlinear fiber, because it has direct effects on pulse broadening, walk-off and phase-matching conditions [23], thus determining the bandwidth and energy requirement of the device to which the fiber is applied. The total chromatic dispersion is separated into two parts: material dispersion and waveguide dispersion. The former only relies on wavelength in vacuum for certain material, while the latter has relation with both the wavelength in vacuum and the effective refractive index which is gained by simulation.

The total dispersion D_t is approximately a combination of material dispersion D_m and waveguide dispersion D_w, therefore we obtain [24]

$$D_t \cong D_w + D_m \tag{1}$$

Waveguide dispersion D_w is given by [25]

$$D_w = -\frac{\lambda}{c}\frac{\mathrm{d}^2 \mathrm{Re}[n_{\mathrm{eff}}(\lambda)]}{\mathrm{d}\lambda^2} \tag{2}$$

where c denotes the speed of light in vacuum and λ denotes the wavelength of light in vacuum and n_{eff} means the effective refractive index.

Due to the finite number of layers of air holes, leaking of the light of the ring to exterior matrix material is occurring through bridges between air holes, resulting in the confinement loss α, which can be obtained by [26]

$$\alpha = \frac{40\pi \mathrm{Im}(n_{\mathrm{eff}})}{\lambda \ln(10)} \tag{3}$$

Here, λ denotes the wavelength of light in vacuum and n_{eff} means the effective refractive index as well.

3. Simulation and discussion

3.1. Proposed structure

A model is built based on the structure shown in Fig. 1**b**. The refractive index n_2 of the host material (fused silica) is 1.45, while that of air, n_1 is 1. The finite element method (FEM) was employed to analyze the mode properties of the PCF. The advantage of this way is that it can handle PCF with any structure parameters and any arrangement of the air holes. Using the FEM, the electric field distribution in a cross-section can be obtained when the incident beam is a Gaussian beam. Figure 2**a** shows the electric field distributions of an incident beam. Figures 2**b** and 2**c** show the electric field distribution of a beam propagating in proposed PCF by 3D and 2D separately.

Comparing Fig. 2**a** with Fig. 2**b**, it turns out that the incident Gaussian beam is shaped into a circular HB, whose main electric field region is a circular ring, rather

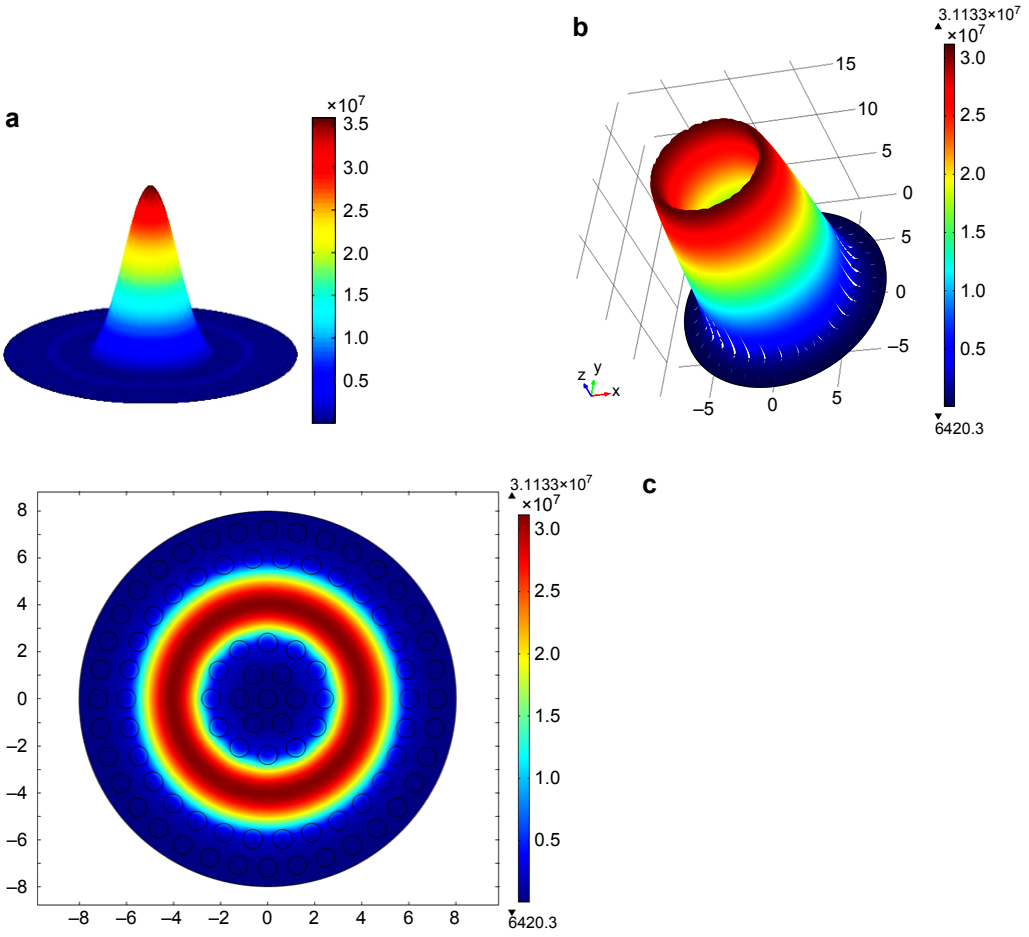

Fig. 2. Electric field distribution of proposed structure (see text for explanation).

than a disc. From Fig. 2**c**, it can be easily observed that the electric field of a beam propagating in proposed PCF is almost wholly confined to the ring-shaped core. Compared with the simulation result in [17, 22], whose HB shape is hexagonal, a circular HB is more suitable for space optical communication systems to avoid the loss of energy caused by the subreflector center reflection in the optical antenna. The transmission efficiency in the optical communication system will be greatly enhanced.

To study the influence of a ring-shaped core size on circular HB dimension, three structures are considered and discussed. The three structures are the same in the parameter setting of $\Lambda = 1.2$ μm and $r = 0.4$ μm, so as materials. The only difference among them is size and position of the defect. One is formed by removing the third and the fourth rings of air holes, as is shown in Fig. 1**b**. Similarly, the other two are formed by removing the second and the third rings, the second to the fourth rings respectively. In order to state conveniently, they were named r_{34}, r_{23} and r_{234} in order.

In [19], DSS is defined as the full-width half-maximum (FWHM) of the radial intensity distribution of HB. Parameter W_{DHB} is the full-width of the maximum intensity times e^{-2}. And r_0 is half of the distance between two peak values. Then the width of the hollow beam W_r can be obtained by the following equation: $W_r = W_{\mathrm{DHB}} - 2r_0$. The normalized intensity distribution of the fundamental mode in above three structures is illustrated in Fig. 3. Images of the corresponding PCF profile are placed in each

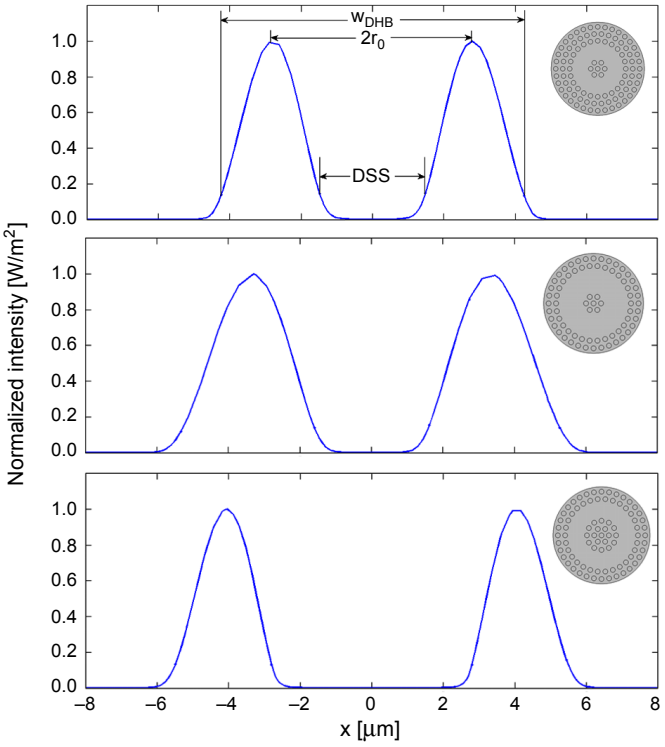

Fig. 3. Normalized intensity of HB generated by corresponding structure.

T a b l e 1. Dimension parameter of HB.

	DSS [μm]	$2r_0$ [μm]	W_{DHB} [μm]	W_r [μm]
r_{23}	2.9646	5.5908	8.4903	2.8996
r_{234}	3.2185	6.5978	10.3275	3.7298
r_{34}	5.6000	8.0582	10.9278	2.8696

subgraph, they are r_{23}, r_{234} and r_{34} from top to the bottom. In the first subgraph, indicators W_{DHB}, $2r_0$ and DSS have been marked using arrows.

Dimension parameter of HB generated by the three structures was obtained by data processing, which is shown in Table 1. It can be seen from the Table that r_{234} reaches maximum in W_r, meanwhile, r_{23} and r_{34} achieve minimum and maximum as to DSS. Obviously, there is a positive correlation between the annular core width and HB width, as with the annular core internal diameter and HB internal diameter. Though not a direct proportion, this rule can still be a guideline when PCFs are designed to generate a circular HB with certain dimension.

Then the core size influence on chromatic dispersion was also studied by discussing above three structures. Figure 4 shows the effective refractive index n_{eff} of three structures obtained by simulation. It is obvious that n_{eff} is approximate to the refractive index of fused silica n_2. Moreover, n_{eff} of all structures decreases with the increase in wavelength.

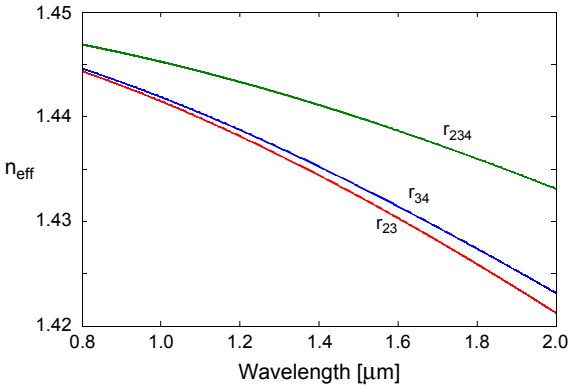

Fig. 4. Effective refractive index *vs*. wavelength.

According to Eqs. (1) and (2), the total dispersion is obtained, shown in Fig. 5. Apparently, for $\lambda = 1.31$–1.55 μm, the wave band of optical communication, the total dispersion is almost within the range of 30–60 ps/km/nm for each structure, which is far from ideal on account of being large and not flat.

However, it has also been found that the total dispersion D_t remains about the same in above three structures. That is to say, when the annular core dimension is changed aiming to obtain a circular HB with required dimension, the effect of resizing on dispersion characteristics could be ignored. Thus more attentions will be focused on dimen-

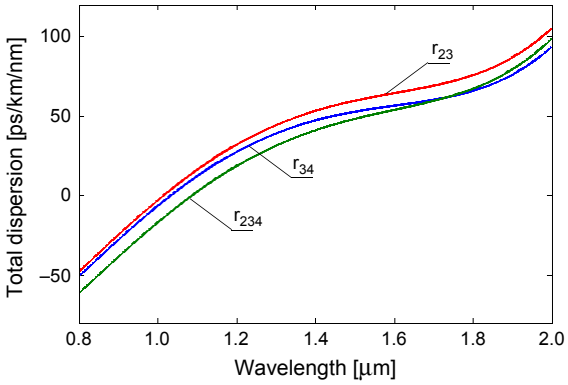

Fig. 5. Total dispersion curve in a broad wavelength range.

sional requirement of the generated HB in its early design phases. As to the management of dispersion, an optimized structure will be studied in the following section.

3.2. Optimized structure and analysis

For the sake of a more flexible and precise management of chromatic dispersion, the proposed structure above was optimized by punching a circle of air holes in the middle of the ring-shaped core, whose radius R is adjustable and much smaller than the radius of other air holes, as is shown in Fig. 5. Other parameters are the same as above, namely, $\lambda = 1.2$ μm, $r = 0.4$ μm, $n_1 = 1$ and $n_2 = 1.45$. Absolutely, the structure in Fig. 1**b** can be regarded as a special case of the structure in Fig. 6, namely, $R = 0$. Based on recent researches [27, 28], electron beam lithography (EBL) can be used to run a super-fine process of 0.1–0.25 μm, with an error of tens of nanometers. This method can satisfy basically the requirements of our design.

Figures 7**a** and 7**b** show the electric field distribution of optimized structure based on Fig. 3 in 2D and 3D, respectively. It can be seen that the optimized structure has an equally good performance in beam shaping, only with difference in electric field distribution of the annular core region.

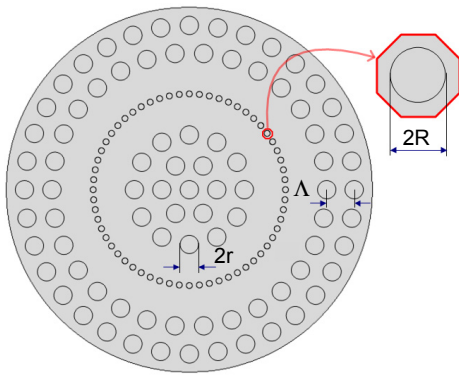

Fig. 6. Cross-section of optimized structure.

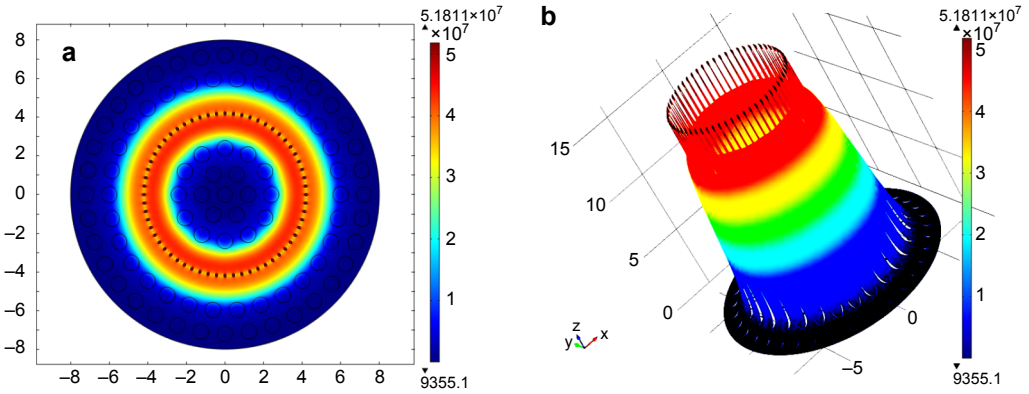

Fig. 7. Electric field distribution of optimized structure (see text for explanation).

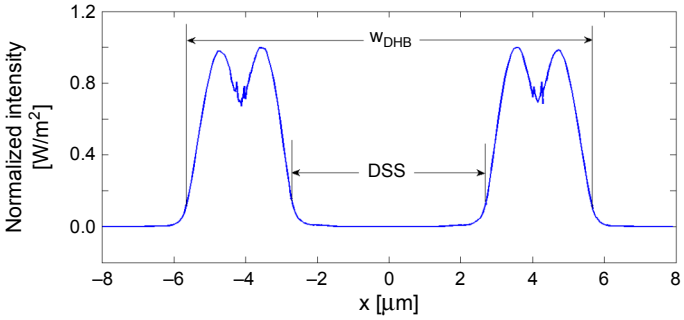

Fig. 8. Normalized intensity of HB generated by optimized structure.

The normalized intensity distribution of the fundamental mode in optimized PCF is illustrated in Fig. 8. Dimension parameters W_{DHB} and DSS are marked in the figure as well. Compared to above three structures in Fig. 3, it can be found that HB generated by the optimized structure has four peaks. This phenomenon may be explained by the added air holes in an annular core, which tends to divide the annular core into two coaxial rings. Therefore, the incident beam tends to converge in the two ring-shaped parts simultaneously. The change is obvious, however, it has little effect on the dimension of the generated HB. Owing to the change of HB shape, above computing method is not applicable. Instead, HB width can be calculated by the equation $W_r = (W_{\mathrm{DHB}} - \mathrm{DSS})/2$. Here, the values of W_r and DSS are 2.9426 μm and 5.4205 μm separately, being nearly identical with those of r_{34} in Table 1. In conclusion, adding air holes in the annular core impacts on the HB dimension slightly.

To study the chromatic dispersion change rule *vs*. wavelength with different structural parameters, the parameter R in model B was set a series value of 0.05, 0.07, 0.09, 0.10, 0.12, 0.14, 0.16, 0.18 and 0.20 μm, respectively.

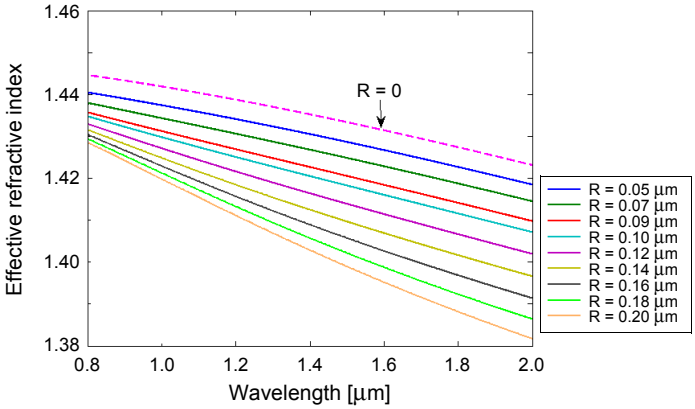

Fig. 9. Effective refractive index *vs*. wavelength.

Figure 9 shows the effective refractive index n_{eff} *vs*. wavelength of the designed PCF with all parameter settings obtained by simulation. The dashed line represents the case of $R = 0$. It is obvious that n_{eff} decreases with the increase in the wavelength λ in an irregularly varying slope in all cases.

The relation between the waveguide dispersion D_w of the designed PCF and the wavelength λ is described in Fig. 10, according to Eq. (2). Meanwhile, the abstract of material dispersion $-D_m$ with different wavelength λ is calculated based on the Sellmeier equation, drawn in Fig. 8 as well. Since the total dispersion D_t is regarded as a linear combination of waveguide dispersion and material dispersion, based on Eq. (1), the points where the waveguide dispersion curve and the abstract of material dispersion curve intersected indicate the case of zero dispersion. That is to say, the corresponding horizontal axis values represent zero dispersion wavelength. All the points are marked by red dots. It can be found that the zero dispersion wavelength increases with the pa-

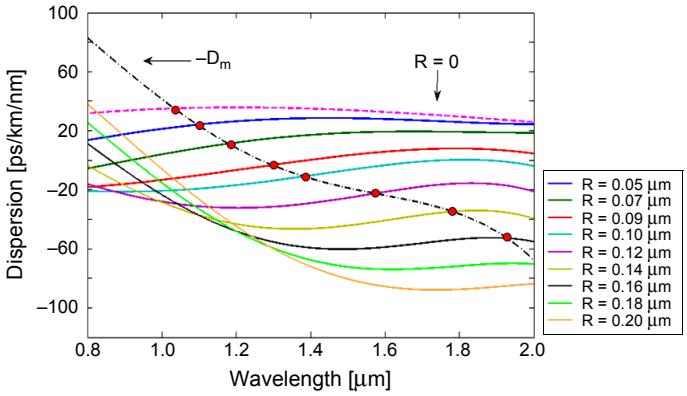

Fig. 10. Waveguide dispersion curve in a broad wavelength range.

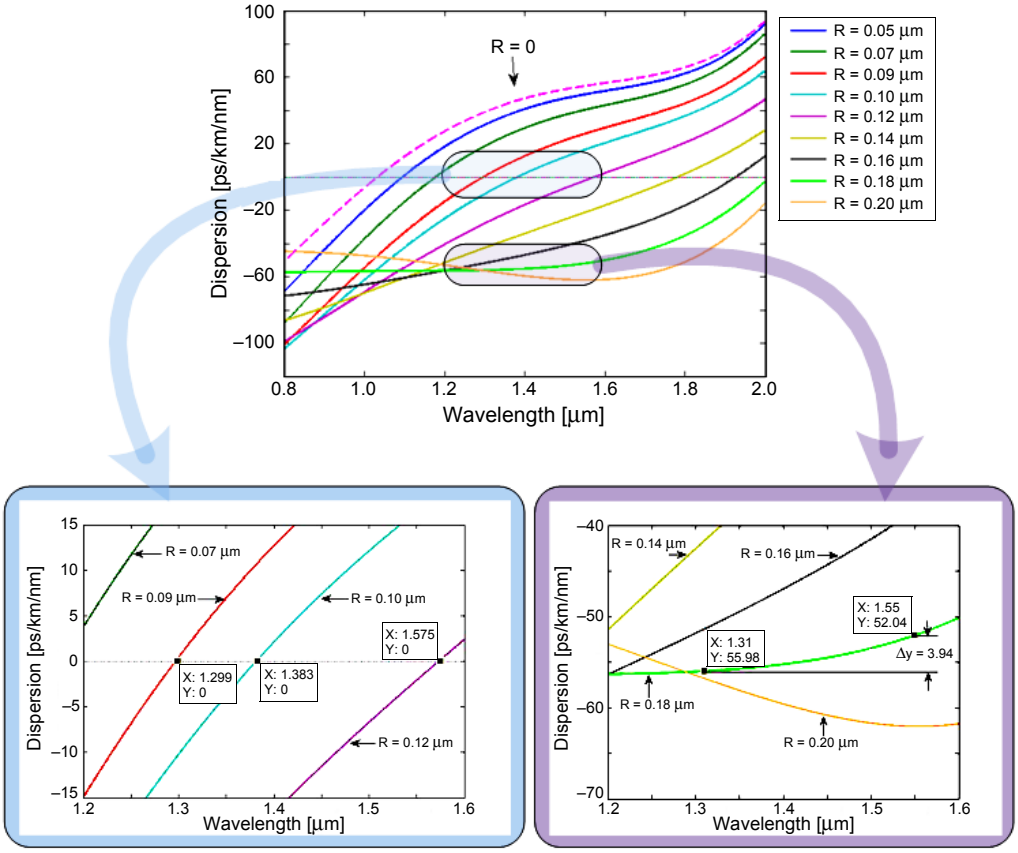

Fig. 11. Total dispersion curve in a broad wavelength range.

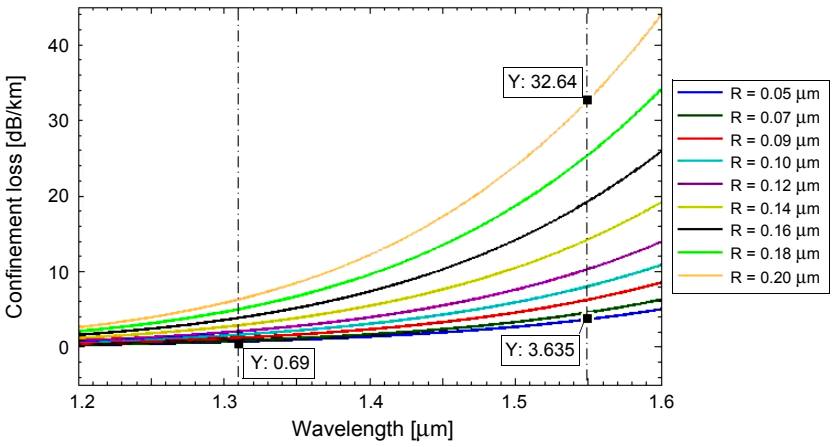

Fig. 12. Confinement loss *vs*. wavelength for different defect structures.

rameter R varying from 0 to 0.20 μm. Therefore, adjusting the parameter R is an effective and precise way to manage zero dispersion wavelength flexibly.

To acquire more intuitive results, a linear combination of material and waveguide dispersion is conducted. Hence, the total dispersion D_t is obtained, shown in Fig. 11. Apparently, for R = 0.09, 0.10 and 0.12 μm, the dispersion wavelength is 1.299, 1.383 and 1.575 μm, respectively, approximate to the universe wavelength of optical communication, 1.31 μm and 1.55 μm, which is a quite important character for optical communication. Furthermore, Fig. 11 shows that the flatness of the total dispersion curve varies with different values of the parameter R. Most noticeably, in the case of R = 0.18 μm, the difference in total dispersion is merely 3.94 ps/km/nm when the wavelength λ is spanning from 1.31 to 1.55 μm, revealing a fairly good quality of optical transmission.

For the models built above, the confinement loss was figured out on the basis of Eq. (3). The results shown in Fig. 12 manifest that the confinement loss increases with the rise of the wavelength λ when the value of the parameter R is determined. The confinement loss falls from 32.64 to 3.635 dB/km when the parameter R ranges from 0.20 to 0.05 μm, reflecting the rule that the confinement loss increases with the rise of the parameter R for the same wavelength λ. In the case of R = 0.05 μm, the losses are 0.69 and 3.635 dB/km for λ = 1.31 μm and λ = 1.55 μm, respectively, approaching to zero. Hence, the structure can be designed feasible to propagate a light beam.

It can be seen from the above analysis that the optimized design achieves the expected objective. In this design, HB dimension and dispersion characteristics are controlled by two different parameters. The size of a ring-shaped core decides about HB dimension in the main, and the radius of air holes in the annular core can manage dispersion flexibly. Considering those designs in [17], a good dispersion characteristic has been obtained. But the dispersion is controlled by core shape and size, and HB is merely a by-product generated sometimes. So generating a HB with required dimension may result in unsatisfied dispersion characteristics. By the above comparison, it is obvious that the optimized design behaves better and flexibly.

4. Conclusion

A new PCF with an annular core has been proposed, which is effective on shaping a Gaussian beam into a circular HB. The shaping effects are confirmed by analyzing the electric field distribution of the cross-section. Dimension of the generated HB has been defined and calculated. Moreover, an effective method to manage the dispersion characteristics has been proposed which has little effect on the dimension of the generated HB. Using this method assures the primary requirement that the generated HB dimension remains nearly the same. Moreover, it is of remarkable flexibility of adjusting chromatic dispersion and confinement loss by slightly altering a certain structure parameter to meet the demands on practical applications, zero dispersion or flattened dispersion in a specific wavelength range. In particular, the minimum value

and optimum flatness of chromatic obtained by the proposed method are good and of high applicability, such as 1.802 ps/km/nm with $\lambda = 1.31$ μm and $R = 0.09$ μm. Owing to these good properties, the design proposed in this paper is applicable to optical communication systems.

Acknowledgements – This work is supported by the National Natural Science Foundation of China under Grant No. 61271167 and No. 61307093, and also supported by the Research Foundation of the General Armament Department of China under Grant No. 9140A07040913DZ02106.

References

[1] KNIGHT J.C., BIRKS T.A., RUSSELL P.S.J., ATKIN D.M., *All-silica single-mode optical fiber with photonic crystal cladding*, Optics Letters **21**(19), 1996, pp. 1547–1549.

[2] BIRKS T.A., KNIGHT J.C., RUSSELL P.S.J., *Endlessly single-mode photonic crystal fiber*, Optics Letters **22**(13), 1997, pp. 961–963.

[3] BIRKS T.A., MOGILEVTSEV D., KNIGHT J.C., RUSSELL P.S.J., *Dispersion compensation using single--material fibers*, IEEE Photonics Technology Letters **11**(6), 1999, pp. 674–676.

[4] FERRANDO A., SILVESTRE E., MIRET J.J., ANDRÉS P., *Nearly zero ultraflattened dispersion in photonic crystal fibers*, Optics Letters **25**(11), 2000, pp. 790–792.

[5] ORTIGOSA-BLANCH A., KNIGHT J.C., WADSWORTH W.J., ARRIAGA J., MANGAN B.J., BIRKS T.A., RUSSELL P.S.J., *Highly birefringent photonic crystal fibers*, Optics Letters **25**(18), 2000, pp. 1325–1327.

[6] HANSEN T.P., BROENG J., LIBORI S.E.B., KNUDSEN E., BJARKLEV A., JENSEN J.R., SIMONSEN H., *Highly birefringent index-guiding photonic crystal fibers*, IEEE Photonics Technology Letters **13**(6), 2001, pp. 588–590.

[7] BRODERICK N.G.R., MONRO T.M., BENNETT P.J., RICHARDSON D.J., *Nonlinearity in holey optical fibers: measurement and future opportunities*, Optics Letters **24**(20), 1999, pp. 1395–1397.

[8] MORTENSEN N.A., *Effective area of photonic crystal fibers*, Optics Express **10**(7), 2002, pp. 341–348.

[9] RANKA J.K., WINDELER R.S., STENTZ A.J., *Visible continuum generation in air-silica microstructure optical fibers with anomalous dispersion at 800 nm*, Optics Letters **25**(1), 2000, pp. 25–27.

[10] EGGLETON B.J., KERBAGE C., WESTBROOK P.S., WINDELER R.S., HALE A., *Microstructured optical fiber devices*, Optics Express **9**(13), 2001, pp. 698–713.

[11] FARIBORZ MOUSAVI MADANI, KAZURO KIKUCHI, *Design theory of long-distance WDM dispersion-managed transmission system*, Journal of Lightwave Technology **17**(8), 1999, pp. 1326–1335.

[12] HANSEN K.P., *Dispersion flattened hybrid-core nonlinear photonic crystal fiber*, Optics Express **11**(13), 2003, pp. 1503–1509.

[13] HOO Y.L., JIN W., JU J., HO H.L., WANG D.N., *Design of photonic crystal fibers with ultra-low, ultra--flattened chromatic dispersion*, Optics Communications **242**(4–6), 2004, pp. 327–332.

[14] KRISHNA MOHAN GUNDU, M. KOLESIK, J.V. MOLONEY, KYUNG SHIK LEE, *Ultra-flattened-dispersion selectively liquid-filled photonic crystal fibers*, Optics Express **14**(15), 2006, pp. 6870–6878.

[15] JINGYUAN WANGA, CHUN JIANGA, WEISHENG HUA, MINGYI GAO, *Modified design of photonic crystal fibers with flattened dispersion*, Optics and Laser Technology **38**(3), 2006, pp. 169–172.

[16] ZHAO-LUN LIUA, XIAO-DONG LIU, SHU-GUANG LI, GUI-YAO ZHOU, WEI WANG, LAN-TIAN HOU, *A broad-band ultra flattened chromatic dispersion microstructured fiber for optical communications*, Optics Communications **272**(1), 2007, pp. 92–96.

[17] RAKHI BHATTACHARYA, SWAPAN KONAR, *Dual-core photonic crystal fibers for dispersion compensation*, Journal of Nanophotonics **6**(1), 2012, article 063520.

[18] SCADUTO L.C.N., SASIAN J., STEFANI M.A., JARBAS CAIADO DE CASTRO NETO, *Two-mirror telescope design with third-order coma insensitive to decenter misalignment*, Optics Express **21**(6), 2013, pp. 6851–6865.

[19] XIAO-XIA ZHANG, SHU-GUANG LIN, SHUO LIU, YING DU, XING-PING ZHU, *Generation of hollow beam from photonic crystal fiber with an azimuthally polarized mode*, Optics Communications **285**(24), 2012, pp. 5079–5084.
[20] KNIGHT J.C., *Photonic crystal fibers*, Nature **424**, 2003, pp. 847–851.
[21] SAITOH K., FLOROUS N., KOSHIBA M., *Ultra-flattened chromatic dispersion controllability using a defected-core photonic crystal fiber with low confinement losses*, Optics Express **13**(21), 2005, pp. 8365–8371.
[22] SHUGUANG LI, XIAOXIA ZHANG, AGRAWAL G.P., *Characteristics of photonic crystal fibers designed with an annular core using a single material*, Applied Optics **52**(13), 2013, pp. 3088–3093.
[23] FEROZA BEGUM, YOSHINORI NAMIHIRA, S.M. ABDUR RAZZAK, SHUBI KAIJAGE, NGUYEN HOANG HAI, TATSUYA KINJO, KAZUYA MIYAGI, NIANYU ZOU, *Design and analysis of novel highly nonlinear photonic crystal fibers with ultra-flattened chromatic dispersion*, Optics Communications **282**(7), 2009, pp. 1416–1421.
[24] DAVIDSON D., *Optical-Fiber Transmission*, [Ed.] Basch E.E.B., Howard W. Sams & Co, 1987.
[25] CHAUDHARI C., SUZUKI T., OHISHI Y., *Chalcogenide core photonic crystal fibers for zero chromatic dispersion in the C-band*, Optical Fiber Communication Conference, OSA Technical Digest (CD), 2009, paper OTuC4.
[26] KUHLMEY B.T., NGUYEN H.C., STEEL M.J., EGGLETON B.J., *Confinement loss in adiabatic photonic crystal fiber tapers*, Journal of the Optical Society of America B **23**(9), 2006, pp. 1965–1974.
[27] DEROSE G.A., LIN ZHU, POON J.K.S., YARIV A., SCHERER A., *Electron-beam lithography techniques for micro- and nano-scale surface structure current injection lasers*, CLEO, 2007, CThN7.
[28] SANABIA J.E., BURCHAM K.E., KLINGFUS J., PIASZENSKI G., KAHL M., JEDE R., *Fixed beam moving stage electron beam lithography of waveguide coupling device structures*, CLEO, 2012, CM4L.3.

Received February 25, 2014
in revised form June 4, 2014